How Many Gradients are Sufficient in High-Angular Resolution Diffusion Imaging (HARDI)?

Liang Zhan[1], Ming-Chang Chiang[1], Alex D. Leow[1], Siwei Zhu[2], Marina Barysheva[1], Arthur W. Toga[1], Katie L. McMahon[3], Greig I. de Zubicaray[3], Matthew Meredith[3], Margaret J. Wright[4], Paul M. Thompson[1]

[1] Laboratory of Neuro Imaging, Department of Neurology, UCLA School of Medicine, Los Angeles, CA, USA
[2] Dept. of Mathematics, UCLA, Los Angeles, CA, USA
[3] Functional MRI Laboratory, Centre for Magnetic Resonance, University of Queensland, Brisbane, Australia
[4] Queensland Institute of Medical Research, Brisbane, Australia

Abstract. We scanned 61 healthy adults with 105-gradient HARDI at 4 Tesla, and examined how the number of diffusion gradients affects the signal-to-noise ratio (SNR) for several common DTI-derived scalar measures: the fractional and relative anisotropy (FA, RA) mean diffusivity (MD), and volume ratio (VR). HARDI applies diffusion-sensitive magnetic field gradients to the brain at a range of spherical angles (typically >100) to analyze white matter microstructure and integrity. We optimized the angular distribution energy on gradient image subsets of size $1 \leq N \leq 94$, to artificially reduce the angular sampling. 7 gradients are mathematically sufficient to determine FA/RA/MD/VR, but by increasing the number of diffusion-sensitized gradients from 20 to 94, SNR improved by 69.23% and 19.93% for VR and RA, and by 12.24% and 8.77% for FA and MD. Measures involving products of 3 eigenvalues (e.g., VR) were noisier, requiring more gradients to determine. FA SNR rose rapidly with more gradients than are routinely collected, suggesting advantages of HARDI even for standard neuroscientific studies.
Keywords: High-Angular Resonance Diffusion Imaging, fractional anisotropy, relative anisotropy, mean diffusivity, volume ratio, Signal-to-Noise ratio**.**

1 Introduction

High-angular resolution diffusion imaging (HARDI) is a powerful extension of MRI, based on applying diffusion-sensitized gradients to the brain in 100 or more different directions. This can quantify anisotropic water diffusion in brain tissue, providing exquisite insight into local fiber orientation and integrity. Many early diffusion imaging studies used the *diffusion tensor* model [1], which describes the anisotropy of water diffusion in tissues by estimating, from a set of K diffusion-sensitized images, the 3x3 covariance matrix of a Gaussian distribution. Each voxel's signal intensity in the k-th image is decreased, by water diffusion, according to the Stejskal-Tanner equation [2]: $S_k = S_0 \, exp\,[-b\mathbf{g}_k^T \mathbf{D}\, \mathbf{g}_k]$, where S_0 is the non-diffusion weighted signal intensity, D is the 3x3 diffusion tensor, $\mathbf{g}_k$ is the direction of the diffusion gradient and b is Le Bihan's factor containing information on the pulse sequence, gradient strength, and physical constants. Although only 7 gradients are mathematically sufficient to determine the diffusion tensor, MRI protocols with higher angular and radial resolution (e.g., HARDI) have been proposed to resolve more complex diffusion geometries that a single tensor fails to model, e.g. fiber crossings and intermixing of tracts.

Recent technical advances have made HARDI more practical. A 14 minute scan can typically sample over 100 angles (with 2 mm voxels at 4 Tesla). HARDI's improved signal-to-noise ratio can be used to reconstruct fiber pathways in the brain with extraordinary angular detail, identifying anatomical features, connections and disease biomarkers not seen with conventional MRI. If more angular detail is available, fiber orientation distribution functions (ODFs) can be reconstructed from the raw HARDI signal using deconvolution methods [3,4], yielding mathematically rich models of fiber geometries using probabilistic mixtures of tensors [5, 6], fields of von Mises-Fisher mixtures [7], or higher-order tensors (i.e., 3x3x…x3 tensors) [8,9]**.** Recent work on stochastic tractography [10, 11] has also exploited the increased angular detail in HARDI, and fluid registration methods have also aligned HARDI ODFs using specialized Riemannian metrics [12].

Ironically, most clinical studies with diffusion imaging still rely on simple scalar measures, such as fractional anisotropy (FA) or mean diffusivity (MD), which can be computed from the diffusion tensor approximation. FA poorly reflects the multidimensional complexity of the ODF, but it is sensitive to white matter deterioration in aging and neurodegenerative diseases, so many clinical studies have concluded that it is unnecessary to collect many more than the 7 gradient images that suffice to determine the diffusion tensor uniquely. Given the trade-off between the available signal-to-noise (SNR) and the time required to collect more gradient images, some studies argue that 20 gradient directions are sufficient to accurately compute FA [13,14], and such acquisition protocols are now typical. Here we aimed to determine whether this is optimal, by examining the signal-to-noise gains, for different standard diffusion-tensor derived indices (FA/MD/RA/VR), with the increased gradient numbers in HARDI. Although simulations suggest that SNR will increase with increasing gradient numbers in DTI [15-17], simulations may not represent the achievable SNR, as many sources of noise (e.g., subject motion, physiological sources of noise, susceptibility of real brain tissue) can only be modeled by empirically studying a population. As such, we scanned 61 subjects with 105-gradient HARDI, providing practical information on real human data that has not previously been available.

2 Materials and Methods

2.1 Subjects and image acquisition

105-gradient HARDI data were acquired from 61 healthy adult subjects (age: 24.5±1.4SD years; 29 men/32 women) on a 4 Tesla Bruker Medspec MRI scanner using an optimized diffusion tensor sequence [16, 18]. 105 images were acquired: 11 baseline (b_0) images with no diffusion sensitization (i.e., T2-weighted images) and 94 diffusion-weighted images (b-value 1159 s/mm^2) in which gradient directions were evenly distributed on the hemisphere [2]. Imaging parameters were: TE/TR 92.3/8250 ms, 55 x 2mm contiguous slices, FOV = 23 cm. The reconstruction matrix was 128 x 128, yielding a 1.8x1.8 mm^2 in-plane resolution. The total scan time was 14.5 minutes.

2.2 Data processing

HARDI data for all 61 subjects were loaded into MedINRIA, a DTI analysis program developed by the INRIA research project *Asclepios* [19]. MedINRIA provides state-of-the-art algorithms for tensor reconstruction and denoising, with a simple user interface and triaxial/3D viewer (http://www-sop.inria.fr/asclepios/software/MedINRIA; **Figure 1**). To eliminate extracerebral tissues, a subject-specific binary mask of the brain was created based on a Partial Volume Classification (PVC) of the corresponding registered 3D T1-weighted structural images [20] and aligned by 9-parameter transformation to the corresponding diffusion tensor images.

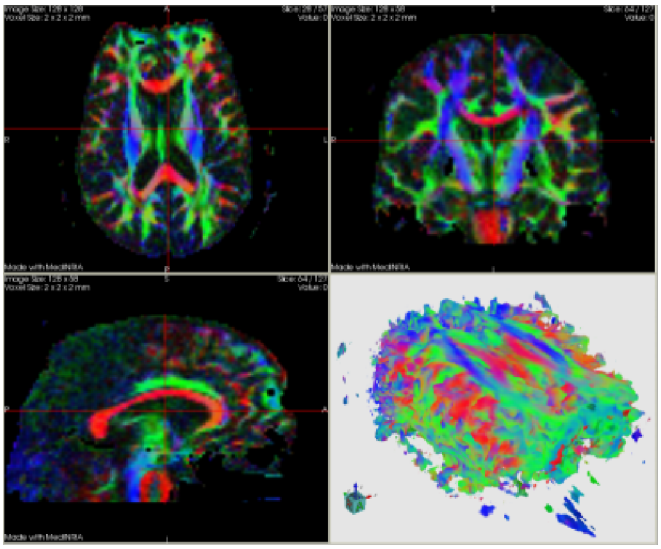

Figure 1. Tensor Reconstruction and Eigenstructure Visualization from HARDI. The 105 gradient images per subject were reconstructed using a tensor approximation at each voxel. The diffusion tensor eigenvalues were retained to compute the scalar diffusion parameters FA/MD/RA/VR. Here the RGB color code indicates the normalized principal eigenvector

direction (x,y,z) of the local diffusion tensor, showing that the HARDI sequence resolves fiber geometry and orientation in detail (red colors show the *corpus callosum*; *bottom left*).

In the Diffusion Tensor (DT) model, a tensor is fitted at each voxel to the set of diffusion images, and maps of indices sensitive to fiber integrity such as fractional or relative anisotropy (FA, RA), mean diffusivity (MD) or volume ratio (VR), may be computed from the tensors' eigenvalues (λ_1, λ_2, λ_3). [18] pointed out that the performance of FA and MD estimation depends on the tensor estimation method. In MedINRIA, a Log-Euclidean (LE) metric is used for tensor estimation, in which matrices with null or negative eigenvalues are at an infinite distance from any positive definite matrix. For each subject, DT images (denoted by $D_{ij,}$ $1 \leq i, j \leq 3$) and FA, RA MD, and VR maps were computed from the HARDI signals standard formulae (**Equation 1**).

$$
\begin{aligned}
FA &= \sqrt{\frac{3}{2}\left(\frac{(\lambda_1-\hat{\lambda})^2+(\lambda_2-\hat{\lambda})^2+(\lambda_3-\hat{\lambda})^2}{\lambda_1^2+\lambda_2^2+\lambda_3^2}\right)} \\
MD &= \frac{\lambda_1+\lambda_2+\lambda_3}{3} \\
RA &= \sqrt{\frac{(\lambda_1-\lambda_2)^2+(\lambda_1-\lambda_3)^2+(\lambda_2-\lambda_3)^2}{2(\lambda_1+\lambda_2+\lambda_3)^2}} \\
VR &= \frac{\lambda_1\lambda_2\lambda_3}{\bar{\lambda}^3} \\
\bar{\lambda} &= \frac{\lambda_1+\lambda_2+\lambda_3}{3}
\end{aligned}
\qquad \textbf{(1)}
$$

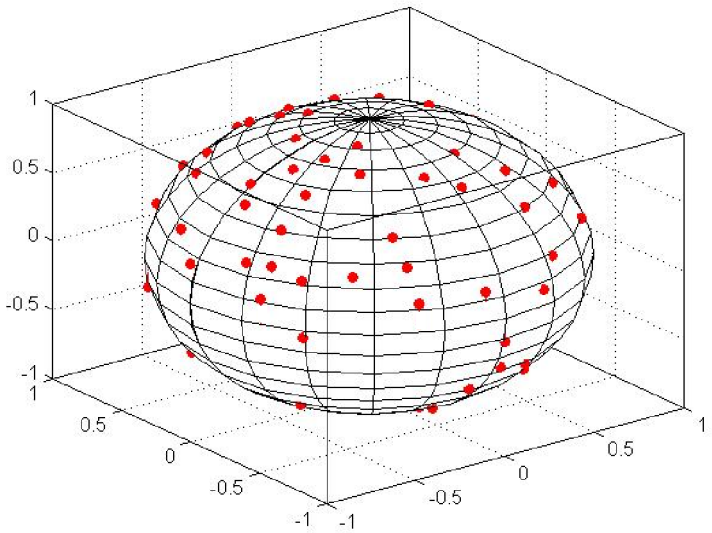

Figure. 2. Spherical distribution of angles at which diffusion-sensitized gradient images were collected, for the 105-gradient HARDI sequence. Each red dot represents one gradient image.

We artificially reduced the angular sampling of the 105-gradient sequence by optimizing the angular distribution energy [2] on subsets of size $1 \leq N \leq 94$ of the diffusion-sensitized gradient images. Since each gradient image is applied in a direction that may be represented as one point (a_i, $1 \leq i \leq 105$) on the surface of the unit sphere (**Figure 2**), the optimality of a gradient vector set is typically defined using PDEs based on electrostatic repulsion, or based on summed spherical distance metrics that attempt to maximize the distance between points on the sphere. Although other approaches are possible (see [22]), in our formulation, we optimized the angular distribution energy by maximizing the summation of the least distances between all points in the Riemannian manifold (**Equation 2**). In Equation 2, a_i and a_j represent two different points on the unit spherical surface.

$$\mathrm{E} = argmax\left(\sum_{i=1}^{105}\sum_{j=1}^{105} argmin\left(distance_R(a_i, a_j)\right)\right) \quad (i \neq j) \qquad (2)$$

For each subject and angular resolution ($1 \leq N \leq 94$), we computed SNR for the FA, MD, RA and VR maps by using all optimized gradient subsets and all 11 baseline (b_0) images, to measure SNR effects with a constant number of b_0 images (this conservative approach slightly favors sequences with fewer gradients, for which fewer than 11 baseline images would typically be collected). Each map's SNR was defined as the ratio of the mean voxel value to the standard deviation of the voxel values. Although this definition does subtract the biological variation in DTI-derived signal across the brain, that component of variation may be assumed constant for all gradient subsets ($1 \leq N \leq 94$), and is therefore not a confound when comparing SNR across gradient numbers. We preferred this approach over selecting a relatively homogeneous region or subset of voxels for our computations; we acknowledge that alternative SNR definitions may be reasonable when specific anatomical tissue classes are the target of study.

3 Results and Discussion

A traditional DTI sequence with a total of 30 gradients might be computed from 27 diffusion-sensitized gradient imaging and 3 baseline images. As we had collected 11 baseline images, to avoid confounding effects we kept the number of b_0 images constant while varying the number of diffusion-sensitized images. Figure 3 shows some representative maps of FA, MD, RA and VR based on HARDI17, HARDI38 and HARDI105 (where the numbers refer to the total number of gradient images).

We found that SNR rose sharply for FA, MD, RA and VR and reached 90% of the available SNR with 22, 19, 31 and 64 of the available 94 diffusion-sensitized gradients. By increasing the number of diffusion-sensitized gradients from 20 to 94, SNR improved by 69.23% and 19.93% for VR and RA, and by 12.24% and 8.77% for FA and MD (**Figure 4**). Measures involving products of 3 eigenvalues (e.g., VR) were noisier, requiring more gradients to determine, but even FA SNR rose rapidly with more gradients than are routinely collected.

HARDI offers increased SNR even for routine brain mapping studies using tensor-derived measures, such as FA, which requires only 7 gradients to determine analytically. Our findings are consistent with studies by Hasan et al. [23], who used bootstrap methods, Monte Carlo simulations and phantom data to show that SNR(RA)/SNR(FA) rises with moderate increases in angular sampling, from 6 to 21. FA and RA are also analytically derivable from each other using closed form formulae, so that the standard deviation of FA, $\sigma(FA)=(1/3)(FA/RA)^3\sigma(FA)$, giving $SNR(FA)/SNR(RA)=3/(3-2FA^2)=1+2RA^2$, if $SNR(FA)=FA/\sigma(FA)$. This means that the maximum SNR advantage SNR(FA)/SNR(RA) is 3 at the highest theoretical anisotropy value (FA=RA=1). Paradoxically, researchers have largely followed the advice that 7-20 gradients suffice to determine F. This reduces acquisition times, but longer acquisitions may provide better SNR not just for tractography but also for routine scalar maps of fiber integrity. Whether or not this increased SNR translates into smaller minimal sample sizes to detect clinically relevant effects depends on the biological variation in these measures across subjects, which deserves further study. Landman et al. [21] also noted that the diffusion tensor orientation (principal eigenvector) depends not just on the angular sampling, but also on patient motion, field inhomogeneity, and EPI-related distortions), and at low SNR, FA measures may not just be noisy, but also biased. Further studies of scanner field strength, spatial resolution, tolerability, motion artifacts, and clinical effect sizes will clarify the added benefit of HARDI's SNR for neuroscientific studies.

4 Conclusions

Based on our current results, more than 20 DWIs should be enough to achieve a satisfactory SNR results for FA, ADC and 30 DWIs for RA, but for VR, more DWIs are needed to improve the SNR.

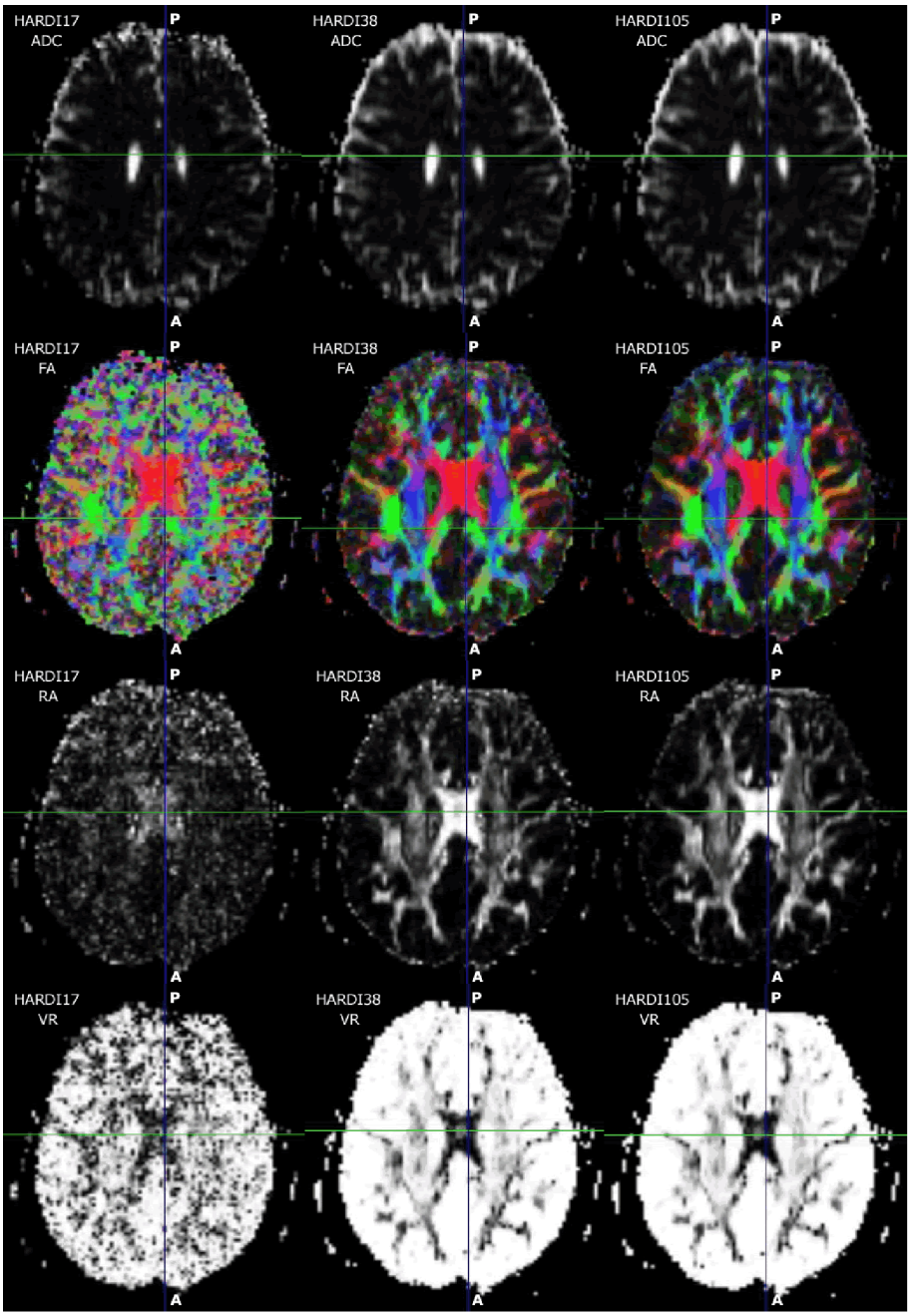

Figure 3. SNR increases for all 4 DTI-derived scalar measures as the number of HARDI gradients is steadily increased. Rows 1-4 show axial slices through the MD map (also known as ADC or average diffusion coefficient), FA map, RA map and VR map. Column 1 is computed from HARDI17 (i.e., the 11 b_0 and 6 non-b_0 images), Column 2 is from HARDI38 (i.e., 27 non-b_0 images), and Column 3 is from HARDI105 (the full protocol of 94 non-b_0 images).

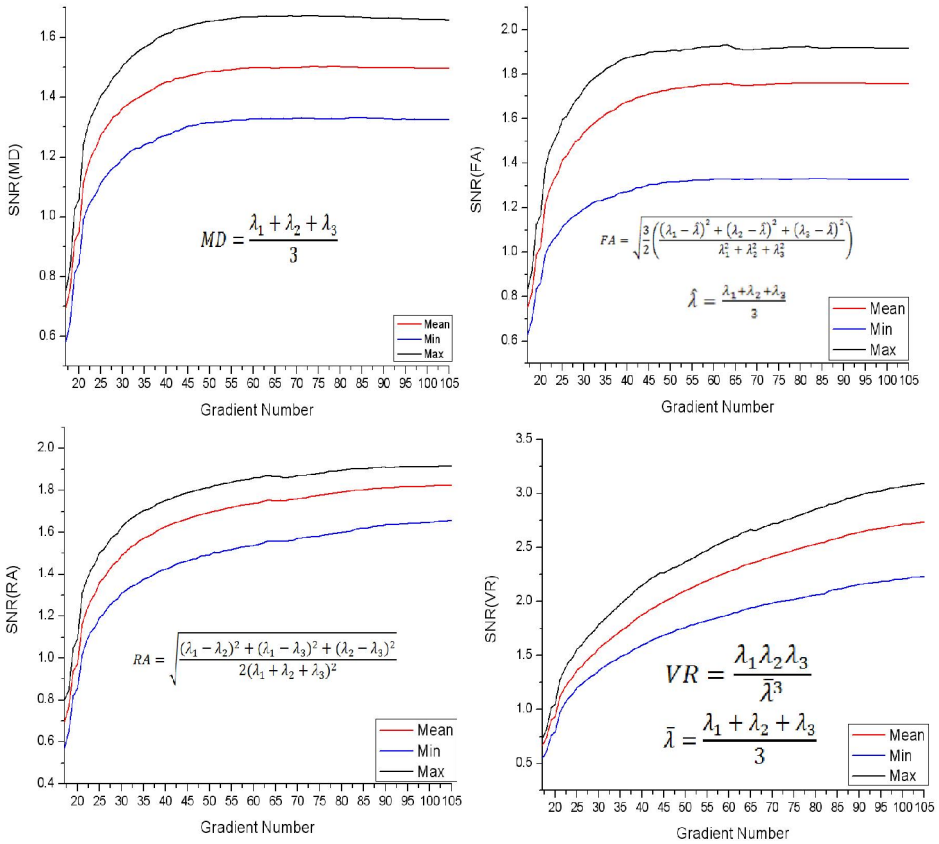

Figure 4. SNR trends with increasing numbers of HARDI gradients. For MD (*top left*), FA (*top right*), RA (*bottom left*), and VR (*bottom right*), the red curves show the average SNR from all 61 subjects, while the top and bottom curves represent the subjects with best and worst SNR. Similar trends appear for the individuals and for the group average SNR. Parameters that involve products of eigenvalues tend to be noisier (e.g., VR), and benefit more from greater angular sampling. The average and individual plots are all monotonically increasing, and FA does not plateau until well beyond the number of gradients typically collected (~20).

References

1. Basser PJ, Pierpaoli C. Microstructural and physiological features of tissues elucidated by quantitative diffusion tensor MRI. J. Magn. Reson., vol. B 111, no. 3, pp.209-219 (1996).
2. Stejskal, EO, Tanner JE. Spin diffusion measurements: spin echoes in the presence of a time-dependent field gradient. J. Chem. Phys. 42:288-292 (1965).
3. Descoteaux M, Angelino E, Fitzgibbons S, Deriche R. A fast and robust ODF estimation algorithm in q-ball imaging. In Third IEEE International Symposium on Biomedical Imaging: from Nano to Macro, pages 81–84, Arlington, Virginia, USA (2006).

4. Tournier JD, Calamante F, Gadian D, Connelly A. Direct estimation of the fiber orientation density function from diffusion-weighted MRI data using spherical deconvolution. NeuroImage, 23:1176–1185, (2004)
5. Jian B, Vemuri BC, Özarslan V, Carney PR, Mareci TH. A novel tensor distribution model for diffusion-weighted MR signal. NeuroImage 37: 164-176. (2007)
6. Leow AD, Zhu S, de Zubicaray GI, Meredith M, Wright M, Thompson PM. The Tensor Distribution Function, ISBI (2008).
7. McGraw T, Vemuri BC, Yezierski B, Mareci T. Von Mises-Fisher mixture model of the diffusion ODF. Biomedical Imaging: Nano to Macro, 3rd IEEE International Symposium on Biomedical Imaging: 65-68. (2006)
8. Ozarslan E, Vemuri BC, Mareci TH. Higher rank tensors in diffusion MRI, Visualization and Image Processing of Tensor Fields, (2005).
9. Barmpoutis A, Vemuri BC. Exponential Tensors: A framework for efficient higher-order DT-MRI computations. In Proceedings of ISBI07: IEEE International Symposium on Biomedical Imaging: Page(s): 792-795. (2007)
10. Perrin M, Poupon C, Rieul B. Validation of q-ball imaging with a diffusion fibre-crossing phantom on a clinical scanner. Phil Trans R Soc Lond B Biol Sci 360:881–891 (2005)
11. Jbabdi S, Woolrich MW, Andersson JLR et al. A Bayesian framework for global tractography. NeuroImage 37:116-129. (2007)
12. Chiang MC, Barysheva M, Lee AD, Madsen SK, Klunder AD, Toga AW, McMahon KL, de Zubicaray GI, Meredith M, Wright MJ, Srivastava A, Balov N, Thompson PM. Mapping Genetic Influences on Brain Fiber Architecture with High Angular Resolution Diffusion Imaging (HARDI), ISBI (2008).
13. Ni H, Kavcic V, Zhu T, Ekholm S, Zhong J. Effects of Number of Diffusion Gradient Directions on Derived Diffusion Tensor Imaging Indices in Human Brain. American Journal of Neuroradiology 27:1776-1781. (2006)
14. Hasan KM., Narayana PA. Retrospective Measurement of the Diffusion Tensor Eigenvalues from Diffusion Anisotropy and Mean Diffusivity in DTI. Magnetic Resonance in Medicine, 56:(1):130-137. (2006)
15. Jones DK. Determining and Visualizing Uncertainty in Estimates of Fiber Orientation from Diffusion Tensor MRI. MRM;49:7-12 (2003)
16. Jones DK, Horsfield MA, Simmons A. Optimal strategies for measuring diffusion in anisotropic systems by magnetic resonance imaging. Magnetic Resonance in Medicine. 42(3): 515-525. (1999)
17. Alexander DC, Barker GJ. Optimal imaging parameters for fiber-orientation estimation in diffusion MRI. Neuroimage 27:357–67 (2005)
18. Pend H, Arfanakis K. Diffusion tensor encoding schemes optimized for white matter fibers with selected orientations. Magnetic Resonance Imaging 25: 147-153. (2007)
19. Pennec X, Fillard P, Ayache N. A Riemannian Framework for Tensor Computing. International Journal of Computer Vision, 66(1):41-66, January 2006. Note: A preliminary version appeared as INRIA Research Report 5255, (2004).
20. Shattuck, D.W. and R.M. Leahy, BrainSuite: an automated cortical surface identification tool. Med Image Anal, 6(2): p. 129-42 (2002)
21. Landman BA, Farrell J.A.D., Smith SA, Mori S, Prince JL. Tradeoffs between tensor orientation and anisotropy in DTI: Impact of Diffusion Weighting Scheme. International Society for Magnetic Resonance in Medicine, 15th Scientific Meeting, Berlin. (2007)
22. Hasan KM, Narayana PA. DTI parameter optimization at 3.0 T: potential application in entire normal human brain mapping and multiple sclerosis research. MedicaMundi 49(1):30-45 (2005).
23. Hasan KM, Alexander AL, Narayana PA. Does fractional anisotropy have better noise immunity characteristics than relative anisotropy in diffusion tensor MRI? An analytical approach. Magn Reson Med;51(2):413–417.(2004)